

1 FOODCHEM-D-18-04215 Manuscript revision

2 Title:

3 Untargeted Mass Spectrometry-Based Metabolomics Approach Unveils Molecular Changes in
 4 Raw and Processed Foods and Beverages

5 Authors:

6 Julia M. Gauglitz^{a,b,c}, Christine M. Aceves^a, Alexander A. Aksenov^{a,b}, Gajender Aleti^d, Jehad
 7 Almaliti^{e,f}, Amina Bouslimani^{a,b}, Elizabeth A. Brown, Anaamika Campeau^{b,g}, Andrés Mauricio
 8 Caraballo-Rodríguez^{a,b}, Rama Chaar^b, Ricardo R. da Silva^{a,b}, Alyssa M. Demko^e, Francesca
 9 Di Ottavio^h, Emmanuel Elijah^{a,b}, Madeleine Ernst^{a,b}, L. Paige Ferguson^b, Xavier Holmes^{a,b},
 10 Alan K. Jarmusch^{a,b}, Lingjing Jiang^j, Kyo Bin Kang^{a,b}, Irina Koester^e, Brian Kwaniⁱ, Jie Li^e,
 11 Yueying Li^e, Alexey V. Melnik^{a,b,c}, Carlos Molina-Santiago^k, Bohan Ni^e, Aaron L. Oom^l,
 12 Morgan W. Panitchpakdi^{a,b}, Daniel Petras^{a,b,c,5}, Robert Quinn^{a,b}, Nicole Sikora^b, Katharina
 13 Spengler^a, Bahar Teke^e, Anupriya Tripathi^{a,b}, Sabah Ul-Hasan^m, Justin J.J. van der Hooft^{a,b,l},
 14 Fernando Vargas^{a,b,n}, Alison Vrbanc^o, Anthony Q. Vu^o, Steven C Wang^{b,n}, Kelly Weldon^{a,b,c},
 15 Kayla Wilson^e, Jacob M. Wozniak^{b,g}, Michael Yoon^b, Nuno Bandeira^{b,p}, Pieter C.
 16 Dorrestein^{a,b,q*}

17 Author Affiliations:

- 18 a. Collaborative Mass Spectrometry Innovation Center, Skaggs School of Pharmacy and
 19 Pharmaceutical Sciences, University of California, San Diego.
- 20 b. Skaggs School of Pharmacy and Pharmaceutical Sciences, University of California,
 21 San Diego
- 22 c. Center for Microbiome Innovation, University of California, San Diego.
- 23 d. Mammalian Genomics, J. Craig Venter Institute, San Diego.
- 24 e. Scripps Institution of Oceanography, University of California, San Diego
- 25 f. Department of Pharmaceutical Sciences, Faculty of Pharmacy, The University of
 26 Jordan, Amman, 11942, Jordan
- 27 g. Department of Pharmacology, University of California, San Diego.
- 28 h. University of Teramo, Faculty of Bioscience, Te, Italy
- 29 i. Bioinformatics Group, Wageningen University, Wageningen, The Netherlands
- 30 j. Department of Family Medicine and Public Health, University of California, San Diego.
- 31 k. Departamento de Microbiología, Instituto de Hortofruticultura Subtropical y
 32 Mediterránea “La Mayora”, Universidad de Málaga, Bulevar Louis Pasteur 31 (Campus
 33 Universitario de Teatinos), 29071 Málaga, Spain.
- 34 l. Department of Medicine, University of California, San Diego

- m. School of Natural Sciences, University of California Merced, Merced, CA, 95343, USA
- n. Division of Biological Sciences, University of California at San Diego, La Jolla, CA
- o. Biomedical Sciences Graduate Program, University of California San Diego, La Jolla, CA, USA
- p. Department of Computer Science and Engineering, University of California, San Diego.
- q. Departments of Pharmacology and Pediatrics, University of California, San Diego.

Abstract:

In our daily lives, we consume foods that have been transported, stored, prepared, cooked, or otherwise processed by ourselves or others. Food storage and preparation have drastic effects on the chemical composition of foods. Untargeted mass spectrometry analysis of food samples has the potential to increase our chemical understanding of these processes by detecting a broad spectrum of chemicals. We performed a time-based analysis of the chemical changes in foods during common preparations, such as fermentation, brewing, and ripening, using untargeted mass spectrometry and molecular networking. The data analysis workflow presented implements an approach to study changes in food chemistry that can reveal global alterations in chemical profiles, identify changes in abundance, as well as identify specific chemicals and their transformation products. The data generated in this study are publicly available, enabling the replication and re-analysis of these data in isolation, and serve as a baseline dataset for future investigations.

Keywords: Untargeted mass spectrometry, Metabolomics, Molecular networking, LC-MS/MS, Food, Fermentation, Tea; Yogurt

60 **1. Introduction:**

61 We consume a variety of foods and beverages during any given day, such as fruits,
62 vegetables, dairy products and meats. The chemical composition of these foods is influenced
63 by factors such as the source, processing method, storage or other handling before
64 consumption, which has been a central focus of the food science field. However, new
65 measurements and data analysis methods can help expand and clarify our understanding of
66 the molecular composition of foods. Within the food science field, there is significant interest
67 and awareness of dietary habits of human populations (Lewis et al., 2009; Schulze et al.,
68 2015-2020 Dietary Guidelines for Americans) and the nutritional composition of food
69 (Thirumdas et al., 2018). Resultant findings can generate policies and nutritional
70 recommendations with the end goal of improving public health (Berger et al, 2019).

71 Mass spectrometry (MS) is an analytical tool that detects ionized molecules and can be
72 used for identification and quantification. The majority of food MS studies employ targeted
73 analysis of a set of predefined compounds via gas and liquid chromatography-mass
74 spectrometry (GC-MS and LC-MS). Many food MS studies monitor chemicals that are harmful
75 when consumed, but the chemical composition of food and its impact on health is not limited
76 to these chemicals (Giorio et al., 2017, Scalbert et al., 2014). Furthermore, the utilization of
77 MS is significant and expected to grow (Yoshimura et al., 2016) in areas such as food
78 monitoring during processing (Marshall et al., 2017), due in part to the cost per data volume of
79 MS having decreased by two orders of magnitude over the past 15 years, and the prediction
80 that it is expected to continue to decrease, presenting MS as a feasible method for large
81 datasets (Aksenov et al., 2017). We present an untargeted approach using liquid
82 chromatography-tandem mass spectrometry (LC-MS/MS) to illustrate the effects of storage

and processing on different food types and, for the first time, pair this methodology with emerging MS-based computational analysis approaches, such as mass spectral molecular networking to assess changes based on processing.

Mass spectral molecular networking enables a broad overview of molecular information that can be inferred from MS/MS data (Watrous et al., 2012). In molecular networking, all identical MS/MS spectra are merged giving a list of unique MS/MS spectra (Watrous et al., 2012). These are then subjected to spectral alignment allowing for spectral matching with offsets based on the precursor mass differences. Molecules generating similar MS/MS spectra are clustered due to similarities in their fragmentation patterns and are referred to as molecular families. A molecular family is a set of MS/MS spectra that are structurally related (Nguyen et al., 2013). In addition, the MS/MS spectra are putatively annotated against reference spectra within the Global Natural Products Social Molecular Networking (GNPS) platform (Yang et al., 2013, Wang et al., 2016). Matches against the reference libraries constitute level 2 or 3 annotations according to the 2007 metabolomics standards initiative (Sumner et al., 2007). The reference libraries that can be searched, as their spectra are publicly available or available for purchase, include: NIST17, Massbank Europe and North America, ReSpect, CASMI, EMBL metabolomics library, HMDB, and GNPS contributed MS/MS spectra (Wang M et al., 2016, Aksenov et al., 2017, Blaženović et al., 2018). The resulting molecular networks visualize chemical relationships of compounds and provide a powerful tool for in-depth interpretation of chemical transformations. One example of this is the use of molecular networking to help characterize a large number of triterpene saponins in Siberian ginseng (Ge et al., 2017)

105 We hypothesize that the untargeted metabolomics approach presented provides
106 information within a gap between targeted molecular analysis and elemental and
107 macronutrient analysis used in food chemistry. We demonstrate the utility of molecular
108 networking and other analysis tools, such as multivariate statistics, in analyzing untargeted
109 metabolomics data collected to assess the chemical impact of food handling techniques. The
110 potential for untargeted mass spectrometry to augment the knowledge of chemical processes
111 was assessed using the following well studied processes: 1) the impact of starter cultures on
112 the fermentation of yogurts, 2) the effects of brewing time on tea, 3) the effect of roasting
113 coffee on molecular composition, 4) how improper meat storage affects changes in chemistry,
114 and 5) how the molecular composition of tomato changes, depending on whether it was
115 ripened on or off the vine or the cultivar selected. All of these scenarios represent typical
116 processing situations that might occur in commonly consumed foods.

117 **2. Materials and Methods:**

118 We provide a general overview of the materials used and methodology for the five food types.
119 Details are provided where these are shared between most sample types - experimental
120 details for each food type as well as brand information can be found in the Supplementary
121 Information S1.1 - S2.2 and Table S1. 702 samples were considered in the final analysis.

122

123 *2.1 Sample collection*

124 Milk, yogurt, tea leaves, brewed tea, coffee beans, brewed coffee, turkey, beef, and tomato
125 were all sampled in duplicate; one replicate was extracted for analysis (see Supplemental
126 Material Table S1.) and the other was archived for future uses. Unique barcode numbers

127 were assigned to each sample. Liquid samples (defined here as milk, brewed tea, and
128 brewed coffee) were collected into two identical empty 2 mL round bottom tubes (Qiagen,
129 Hilden, Germany). All other sample types were collected in 2 mL round bottom tubes pre-filled
130 with 1.0 mL room temperature ethanol-water (95:5 v/v), (ethyl alcohol, pure, 200 proof
131 (Sigma-Aldrich, Saint Louis, MO, USA)) and deionized Water (Invitrogen UltraPure™, Grand
132 Island, NY, USA)). Duplicate samples were collected in empty 2 mL round bottom tubes and
133 archived. Sample tubes were weighed before and after sample collection, unless otherwise
134 noted in the metadata. All samples were stored at -80°C until downstream sample preparation
135 for MS-based metabolomics. **Figure 1** highlights representative examples of images
136 associated with the five food types that were sampled.

137 Pasteurized whole milk (Horizon Organic Vitamin D Milk; Broomfield, CO, USA) and
138 three yogurts (Oikos Plain Greek Nonfat Yogurt (Dannon, Horsham, PA, USA), Voskos Plain
139 Greek Yogurt (Sun Valley Dairy, Sun Valley, CA, USA) and Kroger Plain Nonfat Greek Yogurt
140 (Kroger, Cincinnati, OH, USA)) were sampled in biological triplicates and used to culture three
141 separate batches of home-fermented yogurt, which were sampled over 6 days for a total of
142 126 samples (see section S1.1 for culturing and sampling description). The yogurts from
143 Oikos and Voskos contained the same live active cultures (*S. thermophilus*; *L. bulgaricus*; *L.*
144 *acidophilus*; *Bifidus*; *L. casei*), whereas Kroger contained *L. acidophilus*, *B. bifidum*, and *L.*
145 *casei*.

146 Twelve teas representing six varieties of tea leaves (Oolong, white, black, green, pu'er
147 and matcha green) were purchased (see supplemental for detailed brand information) and
148 sampled in biological triplicate before brewing, 10 water blanks, and at 0.5 min, 1 min, 4 min
149 and 240 min after addition of hot water, giving a total of 185 brewed tea samples.

150 38 unique types of coffee were purchased, representing different roasts, brands, and
151 origins. Coffee beans and brewed coffee were sampled in biological duplicates. There was a
152 total of 152 samples.

153 There was a total of 119 meat samples; two types of turkey (certified organic and
154 conventional) as well as two types of beef (certified organic and conventional) were sampled
155 in biological triplicates over a 5-day time course to investigate meat spoilage. Each meat
156 product was sampled into two petri dishes: one sample was spiked with tetracycline (final
157 concentration of 300 ppb residual tetracycline) while the other was treated with the vehicle
158 (i.e. 70% EtOH). Although tetracycline is used commonly as a growth promoter for livestock in
159 some countries, here, it was added to see the effects of this antibiotic on a 5-day food
160 spoilage test (Granados-Chinchilla & Rodríguez, 2017).

161 120 tomato samples were sampled from 8 different types of tomatoes (3 brands of
162 conventional cherry tomato, 1 organic cherry tomato, 1 home-grown cherry tomato, 1 roma
163 tomato from a San Diego [CA, USA] farmers' market, purchased canned tomatoes and
164 sundried tomatoes) as well as a 5-day ripening time course of organic cherry tomatoes (see
165 Supplemental for detailed brand information). The private garden-grown tomatoes were
166 naturally grown, ripened on the vine and were not treated with any pesticides/herbicides. The
167 farmers' market tomatoes were also indicated as not treated with pesticides/herbicides. We
168 investigated the effect of origin and storage time (at room temperature) on the molecular
169 composition.

170 Samples were collected according to detailed procedures outlined in the
171 Supplementary Information (S1.1 and Table S1.) and depicted in **Figure 1**.

172

173 *2.2 Metadata*

174 Metadata were entered manually for all samples. Images were used to capture key sample
175 information including unique barcode IDs, packaging information and time of sample
176 collection. Metadata consisted of 142 different descriptive categories including but not limited
177 to: ingredients, packaging type, location of food production, location of sample collection,
178 store and brand names, UPC codes, NDB numbers and descriptions, cheese and dairy types,
179 fermented and non-fermented food, botanical definitions and genus names of plant samples,
180 conventional vs organically produced, type of animal meat, and presence of common
181 allergens and additives. Sample information entries were standardized using a metadata
182 dictionary that explained the types of information needed for each category as well as the
183 correct formatting. The metadata spreadsheet and dictionary are publicly available (see Data
184 and Code Availability in Appendix).

185

186 *2.3 Sample processing*

187 All samples were extracted in ethanol, centrifuged, dried by centrifugal evaporation and
188 resuspended in 50% MeOH / 50% Water (Optima LC-MS grade; Fisher Scientific, Fair Lawn,
189 NJ, USA) containing 2µM sulfadimethoxine (Analytical Standard, Sigma-Aldrich), as an
190 injection control. Detailed sample processing information can be found in the Supplemental
191 **Section S1.2**. 5 µL of resuspended extract was injected for LC-MS/MS analysis. Untargeted
192 metabolomics was carried out using an ultra-high-performance liquid chromatography system
193 (UltiMate 3000, Thermo Scientific, Waltham, MA) coupled to a Maxis Q-TOF (Bruker
194 Daltonics, Bremen, Germany) mass spectrometer with a Kinetex C18 column (Phenomenex
195 Torrance, CA, USA). Data were collected using a data dependent acquisition method outlined

196 in the Supplementary Information (**Section S2.1**). Electrospray ionization in positive mode was
197 used. Data were assessed for quality as described in **Section S2.2** prior to data analysis.

198

199 *2.4 Data analyses*

200 *2.4.1 Molecular networking and small molecule annotations*

201 GNPS molecular networking parameters were set to a minimum requirement of 4 ions to match
202 and a cosine score of >0.7 (<https://gnps.ucsd.edu>). Parent mass tolerance was 0.1 Da and MS/MS
203 was set to 0.1 Da (these parameters were used as many reference type spectra are low resolution).
204 The library search was performed with min match peaks of 4 and a cosine >0.7. Due to the different
205 small molecule compositions for each food, the annotations of all individual food analyses were
206 impacted differently, as recently shown with Passatutto, a false discovery rate (FDR) estimator
207 (Scheubert et al., 2017). Passatutto was used to estimate FDR for the annotations with our settings for
208 each of the five sub-analyses. Passatutto uses a decoy database created using fragmentation trees
209 and rebranching of fragments to estimate the FDR. With these analysis parameters, the estimated
210 FDR of annotations, based on spectral matching, at level 3 for the milk to yogurt was 0.5%, 0.2% for
211 tea, 0.09% for coffee, 1.5% for meat, and 4.8% for tomato.

212 For the milk to yogurt analysis, 126 samples resulted in 78,203 MS/MS spectra, of
213 which 63,241 passed the minimal requirement of four ions and minimum of two identical
214 spectra (**Supplementary Figure 6**). After clustering identical spectra 4,142 nodes remained.
215 147 of the nodes had spectral matches against the libraries searched (3.5% annotation rate).
216 185 tea samples resulted in 50,547 MS/MS spectra, 44,505 of which passed filtering
217 (**Supplementary Figure 10-11**). After merging identical spectra, 1,834 unique MS/MS
218 spectra comprised a molecular network with 207 annotations (11.2% annotation rate). 146
219 coffee samples resulted in a total of 50,929 MS/MS spectra. After filtering, 42,752 MS/MS

spectra remained, which condensed to 1,460 unique spectra in **Supplementary Figure 7**. Of the 1,460 unique spectra, 72 had spectral matches to the reference libraries within a cosine of 0.7 (4.9% annotation rate). The meat analysis included 119 samples, resulting in 72,083 MS/MS spectra, 54,663 of which passed the filtering step (**Supplementary Figure 8-9**). Merging all identical spectra resulted in 5,035 unique spectra of which 313 were annotated (6.2% annotation rate). MS of the 120 tomato samples resulted in 71,430 MS/MS spectra, 62,263 passed the filtering for a minimum of 4 ions and a minimum of two identical MS/MS spectra in the dataset, which condensed to 2,611 unique spectra that are presented as nodes (**Supplementary Figure 5**). 212 of the nodes were putatively annotated using the GNPS libraries (8.1% annotation rate). All annotations are level 2 or 3 according to the 2007 metabolomics standards initiative (Sumner et al., 2007).

231

232 2.4.2 Feature finding using mzMINE

233 MS¹ feature detection was performed using mzMINE2 (<http://mzmine.github.io/>). Outputs of
234 the feature matrix report area-under-the-curve. Parameters used for feature finding can be
235 found in Supplemental Materials (**Section S2.3**). Samples that did not contain the internal
236 standard, sulfadimethoxine, were re-injected. MS/MS belonging to the internal standard
237 sulfadimethoxine were observed in all data included in the analysis; this feature was removed
238 from the MS¹ feature table prior to normalization by sample for downstream statistical
239 analyses.

240

241

242

243 2.4.3 Multivariate statistical analysis and visualization

244 We used principal coordinates analysis (PCoA) to observe broad molecular patterns and
245 trends within the data. PCoA takes a dissimilarity matrix as input and aims to produce a low-
246 dimensional graphical representation of data, such that samples closer together have smaller
247 dissimilarity values than those further apart. PCoA plots are a beta diversity metric (diversity
248 between samples) and consist of orthogonal axes where each axis (PC1, PC2, PC3) captures
249 a percentage of the total variance. For PCoA, signal intensities of the MS¹ features were
250 normalized with Probabilistic Quotient Normalization (PQN) (Ejigu et al., 2013). PCoAs were
251 calculated with the Canberra dissimilarity metric using QIIME (Caporaso et al., 2010) and
252 visualized in EMPeror (Vázquez-Baeza et al., 2013).

253 Heatmaps were created from the filtered and preprocessed MS¹ feature tables, comprising
254 both overall features as well as only features with a GNPS library hit. The Jupyter notebooks
255 (R and python) used to create the heatmaps and perform the statistical analyses are publicly
256 available at [https://github.com/DorresteinLaboratory/supplementary-](https://github.com/DorresteinLaboratory/supplementary-MolecularChangesInFood)
257 [MolecularChangesInFood](https://github.com/DorresteinLaboratory/supplementary-MolecularChangesInFood).

258 3. Results & Discussion

259 Untargeted MS revealed molecular differences between food types as well as within a food
260 category due to variations in source and the time-based processing methods of fermentation,
261 brewing, roasting, spoilage, and ripening. A combination of molecular networking, based on
262 MS/MS spectra, multivariate and univariate statistical analysis of MS¹ features, and data
263 visualization with principal coordinate analysis plots and heatmaps augmented current

264 chemical knowledge of these processes, and exemplified molecular differences on a global
265 scale and individually for each food type.

266 *3.1 A beta diversity analysis of food types and their processing*

267 Visualization of the complex beta diversity matrix of our MS¹ data, visualized using
268 PCoA plots, showed clear separation by sample type, which was expected (**Figure 2 and**
269 **movie S1**). Yogurt and milk samples formed distinct groups (blue). Tomato and meat
270 samples formed tight groups, orange and red, respectively, while the tea had two groups
271 representing the solid (tea leaves) and brewed samples (green). Coffee had three groups
272 corresponding to extracts of whole or ground beans, depending on the variety, and brewed
273 coffee. Sample groups that had tighter clustering were more chemically similar, regardless of
274 sample collection and processing. Because dissimilarities within samples were smaller than
275 the dissimilarities between food types, each sample type was processed separately to
276 maximize separations in PCoA space within a single food type.

277 PCoA analysis of the yogurt and milk samples showed separation based on brand,
278 despite the fact that they contained similar live active cultures and ingredients (**Figure 3a**).
279 The home fermentation time courses of milk inoculated with different yogurts, as starter
280 culture, are displayed in **Figure 3b and Figure S1a-S1b**. The fermentation process and
281 associated molecular changes were visualized by all three home ferments becoming more
282 yogurt-like, as illustrated by increases in distance between the Kroger yogurt and the starting
283 milk in PCoA space, corresponding to transition of the home ferment (milk + starter yogurt)
284 through time, becoming more similar to the original starter culture (**Figure 3b**). Voskos
285 contained Grade A pasteurized milk and cream, in addition to nonfat milk found in the Oikos,

possibly contributing to differences between these yogurts and the corresponding home ferments, despite containing the same live active cultures (**Figure 3a, Figure S1a-S1b**).

PCoA analysis of tea samples, **Figure 3c**, revealed unambiguous differentiation of tea leaves and brewed tea, as well as differences between tea types. Note, blank water samples were most differentiated from the solid extract samples along PC1 (**Figure 3c**). Twelve different teas were sampled at 0.5 min, 1 min, and 4 min to explore the brewing process with respect to time and emulate tea that has been left steeping for longer periods of time (240 min). The tea samples, regardless of type, appeared most similar (in PCoA space and hence chemistry) to the water blanks at the earliest time points and became more similar to solid samples over time (along the PC1 axis which explained 25.9% of total variance), reflecting the typical brewing process while measuring empirically the release of compounds from the leaves (**Figure 3c, Figure 3d. Figure S1c**). The kinetics of tea extraction in the PCoA plot shared similar trends for all teas. We observed minor chemical differences between 240 min and 4 min for all tea types, which supports a steeping time rationale that appears to be effective for extraction of phytochemicals from tea. Differences, based on tea type, were also observed: white, green, matcha green, and black tea liquid samples were more similar to each other than to oolong and pu'er, which were differentiated along PC3 (6.81% of total variance) (**Figure 3c**); **Figure 3d and Figure S1c** illustrate clear differences in beta diversity across different American and British teas and Chinese teas (oolong and pu'er), respectively. It is noteworthy that, although PCoA enabled observation of overall trends, it did not display changes in individual molecule concentrations. Individual chemical changes are visualized in section 3.2 (Heatmaps) and discussed in section 3.3 (Molecular Networking and Annotations).

PCoA analysis of coffee revealed a clear trend among the sample types: brewed coffee (left hand side of PCoA) vs ground coffee (right hand side of PCoA) (**Figure S1d**). Besides samples clustering by sample type, different roast types could not be identified using PCoA but, as noted, changes in individual molecules are not captured using this approach. It is possible that molecular changes induced by roasting might be observed predominantly as volatile molecules, which were not assessed in this study. Indeed, changes in aroma, between the different roasting types, could be readily perceived.

Figure S1e-1f shows the effects spoilage had on ground beef and turkey, in the presence and absence of tetracycline, visualized along PC1, 20.88%. A key driver of chemical differences in PCoA was the type of meat (turkey or beef) (**Figure S1e; PC2 8.4%**). As tetracycline is used in the cattle industry, in some countries/ regions, we sought to identify if it also resulted in differences in chemical composition over time, possibly due to changes in microbial colonization and degradation during spoilage. To control for factors such as source and treatment of the meat, we added exogenous tetracycline as a treatment and the vehicle to controls. Samples with and without tetracycline changed similarly over time indicating that, based on the untargeted LC-MS/MS analysis, addition of tetracycline did not greatly impact chemical changes during aging processes (**Figure S1f**).

PCoA analysis of the tomato samples revealed that both source (**Figure S1g**) and storage time (**Figure S1h**) affected the molecular composition of tomatoes. As expected, processed tomato samples (canned and sundried) occupied very different PCoA spaces than fresh tomatoes (**Figure S1g**). Chemical differences between the processed and fresh tomato could be attributed to the contribution of processing (e.g. heating or addition of sugar and oil) as well as packaging materials and not just the chemical compositions of tomatoes. It was

also notable that differences existed for fresh tomatoes, with those from the farmers' market most closely resembling home-grown tomatoes, and all store-bought tomatoes resembling one another, whether organic or not. It is likely that the close similarity of garden and farmers' market roma tomatoes resulted from similar treatment, where the fruits are ripened on the vine and collected and sold without processing, including storage in different types of packing or washing (this is known for the garden tomatoes and presumed for the farmers' market). Conversely, store-bought tomatoes are collected at an early stage, often not fully ripened for ease of transportation, transported over long distances, packaged, and treated with exogenous ethylene (depending on the supplier). This appears to have a more significant effect on the chemical compositions of tomatoes than the "organic" designation. When organic cherry tomatoes were left at room temperature to ripen, their molecular composition changed over time (**Figure S1h**), although the tomatoes did not notably change in either appearance or smell.

3.2 Heatmaps for Identification of Chemical Changes by Food Group

We created heatmaps to visualize molecular changes between samples for time course experiments, specifically brewing tea, yogurt fermentation, tomato ripening, and improper meat storage, and to gain insight into features that behave similarly over time or originate from different sample types.

Complementary to a PCoA, heatmaps provide a visual overview of data to give more detailed information about molecular changes driving differences within and between sample types. **Figure 4** shows tea and milk-to-yogurt time courses, which had the largest changes in abundance; heatmaps for other sample types are included in the Supplementary Information (**Figure S2-S5**). Consistent with the PCoA analysis, we observed different metabolite profiles

354 between tea leaves and brewed tea (**Figure 4a**). Furthermore, we observed an increase in
355 relative intensities of molecular features due to longer brewing times, independent of the tea
356 type. We assessed the correlation of relative intensity per feature and tea type with extraction
357 time, which resulted in a total of 2,045 significantly correlated features (*spearman correlation*,
358 *p-value* < 0.05). For example, we observed that the relative intensities of procyanidin B and
359 theaflavin increased over time (*Kruskal–Wallis*, *N*=6, *p-value* ranging from 0.01 to 0.02,
360 *between brewing times 0.5 and 240*) (**Figure 4b and Figure S6a**). We also assessed the
361 correlation of relative intensity per feature and home ferment with different yogurt inoculums
362 over time. For the Kroger yogurt, this resulted in a total of 1,587 significantly correlated
363 features (*spearman correlation*, *p-value* < 0.05) (**Figure 4c**). **Figure 4d and Figure S6b**
364 highlight selected molecular features for which we obtained putative structure annotations
365 through GNPS library matching. For example, we observed that the relative intensity of 4-O-
366 beta-galactopyranosyl-D-mannopyranose decreased over time for each yogurt type
367 individually as well as overall (*Kruskal–Wallis*, *N*=9, *p-value*=0.0023, *between 0 and 58 hrs*)
368 (**Figure 4d**).

369 Molecular changes during meat (beef and turkey) storage over five days were also
370 visualized using a heat map (**Figure S3a**). When comparing antibiotic- vs non-antibiotic-
371 treated meat (beef and turkey), overall molecular differences, as seen in PCoA space, did not
372 vary. However, there were some specific low intensity molecules that changed, although
373 differences were minimal due to the addition of tetracycline, which was consistent with
374 observations from the PCoA. We observed differences between organic and non-organic
375 beef. For example, in non-organic beef, oleoyl-taurine increased during the 5 days but did not
376 appear in organic samples, while concentrations acetyl-carnitine decreased in non-organic

377 beef but were consistent across all time points for organic beef. In turkey, the rates of
378 appearance of oleoyl-aurine and disappearance of acetyl-carnitine were only slightly different
379 (**Figure S3b**). The spectral match to the fungal molecule, termitomycamide E (Choi et al.,
380 2010), with parent mass difference 0.000 Da and very strong cosine match of 0.84, increased
381 over time. The presence of three analogues, with mass differences pointing to different acyl
382 chain lengths, and suppression with the addition of tetracycline, would be consistent with
383 increased microbial (fungal) loads (**Figure S5**).

384 Molecular differences between tomato samples were most striking when comparing
385 sun dried, canned, and fresh tomatoes. In the heatmap, no clear-cut large-scale patterns
386 were observed when visualizing molecular changes during ripening of fresh tomatoes (**Figure**
387 **S2**). During the ripening process, some individual molecular features were found to decrease
388 in relative abundance. For example, 5'-methylthioadenosine, a key ripening hormone for
389 plants and precursor of plant-produced ethylene (North et al., 2017), was found to have
390 decreased significantly in relative abundance over the 5-day time course. Also, plant
391 flavonoids (including a level-3 annotation for naringenin) and tomatidine, a tomato-specific
392 alkaloid (Brink and Folkers, 1951; Friedman, 2013), were found to have decreased
393 significantly in relative intensity over time. This is informative as many of the health properties
394 associated with consumption of polyphenol-containing foods are attributed to molecules like
395 naringenin and our results, therefore, indicated tentatively that the nutritional value of
396 tomatoes might change over the time period tomatoes are stored in the home environment.

397 *3.3 Molecular networking and identification of known and related compounds*

398 Mass spectral molecular networking provided additional information about molecular
399 relationships that complemented global differences captured by PCoA and further explored

the molecules and molecular changes within each food type. In milk and yogurt, matches with six carbon sugars, disaccharides and oligosaccharides, vitamins, and acylated carnitines were observed (**Figure 5b**). In addition, large lipid molecular families, such as sphingolipids, and glycerol conjugated with fatty acids, such as monoolein and linoleoylglycerol, were identified. Delvolid, also known as the clinical antifungal 'natamycin', which is an additive used to preserve dairy products, was detected (Branen et al., 2001) and did not change in relative abundance over time. These annotations are all consistent with the animal origins of the samples (milk, yogurt). However, we also obtained unexpected annotations. A molecular family of bile acids, containing annotated glycocholic and cholic acids, was identified. This molecular family was not expected to be present in these samples, as they are primarily associated with the gut. Putative assignments were inspected and confirmed using manual inspection of raw data, accurate mass, fragmentation pattern, and retention time analysis, which further supported the presence of this molecular family.

A large range of phytochemicals were annotated in tea samples (**Figure 6c and Supplementary Figure 12**), including large molecular families associated with flavonoids, with spectral matches to puerins, catechins, and apigenin (assignments are putative as isomers are difficult to differentiate in accordance with level 3 metabolite identification (Cuyckens & Claeys, 2004, Sumner et al., 2007, Borges et al., 2018). MS work on tea has been done primarily in negative ionization mode. Here, using the positive ionization mode, we corroborated earlier work finding molecular families containing flavonoid aglycones with MS/MS matches to quercetin, kaempferol, myricetin, and (epi)catechin – glycosides of which are abundant in tea (van der Hooft et al., 2012a) – and a large molecular family consisting of glycoside derivatives that had spectral matches with quercetin and kaempferol that were

423 bundled together with chlorogenic acids. Note, the majority of nodes for this family were
424 annotated with GNPS community contributed library hits, indicating a greater library coverage
425 for some compound classes, likely due to community contributed spectra. As expected,
426 caffeine was also annotated in tea samples. Theaflavin, a polyphenol formed during fungal
427 oxidation and its analogues, often associated with black tea (Zhang et al., 2018), were
428 detected in white, green, black and oolong tea samples. Theaflavin increased in relative
429 concentration over time, as shown in **Figure 4 and Figure S13**. These annotations were
430 consistent with known processes that use polyphenol building blocks to create larger
431 scaffolds like theaflavin and give black tea its typical color. Furthermore, fuzhuanins,
432 polyphenol-derived molecules (Luo et al., 2013), which are beta-ring fission lactones of
433 flavan-3-ols like epicatechin, were found at high abundance in tea samples.

434 In coffee (**Figure 5c**), we also observed caffeine as well as methyl-caffeine (1,3,7,8-
435 Tetramethylxanthine) and another related compound with a delta mass of m/z 14.01 (CH_2),
436 corresponding to theobromine. Furthermore, we detected several flavonoids and a large
437 number of hydroxycinnamic acids and chlorogenic acids, which are commonly observed in
438 plants (Islam et al., 2018; Clifford et al., 2017; Pastoriza et al., 2017; Tajik et al., 2017;
439 Naveed et al., 2018). In addition, library matching revealed the presence of mascarosides,
440 molecules commonly observed upon roasting of coffee (Shu et al., 2014). The mascarosides
441 were identified in the molecular network by m/z 162.053, 15.996 and 18.011 gains and
442 losses, corresponding to mass shifts associated with six carbon sugars, oxygen, and water,
443 respectively – all pointing consistently to the presence of glycosylated mascarosides.

444 In the meat samples (**Figure 6a**), as expected, we observed MS/MS matches to
445 tetracycline displayed as a single node (no related spectra were detected), which were more

446 abundant in turkey samples. Although tetracycline is used commonly as a growth promoter,
447 here it was added to see the effects of this antibiotic on a 5-day food spoilage test (Granados-
448 Chinchilla & Rodríguez, 2017). We also observed spectral matches with carnosine as well as
449 a large cluster of acyl carnitines with five spectral matches to different acylations. The acyl
450 carnitines were observed predominantly in beef. However, we also found a molecular family
451 of N-acyltaurines (NATs), a recently discovered class of lipids (Turman et al., 2008). **Figure**
452 **S3** shows how NAT concentrations increased, after two days of storage at room temperature,
453 whereas levels of acylcarnitines (markers for beta-oxidation) dropped, suggesting these
454 chemical changes were associated with decomposition over time. Ceramides, component
455 lipids in eukaryotic cell membranes, were detected in both beef and turkey, but they only fell
456 below the level of detection after 5 days in beef. Their presence suggested disintegration of
457 cells within the tissue and the lability of ceramides would explain their disappearance over
458 time. Oxidation in the presence of haem-iron may have contributed to increased degradation
459 in red meat compared with turkey. In contrast, a molecular family containing carnosol, a
460 metabolite from rosemary (Loussouarn et al., 2017), was observed in turkey, but not in beef.
461 Only the packaging of turkey grown without antibiotics and growth hormones stated that
462 rosemary was used (see study Metadata), yet it was observed in both conventionally grown
463 as well as antibiotic-free meat. Both dipeptides and *N*-methyl histidine were detected during
464 the 5-day aging process of the meat. Thus, the molecular families described here are
465 consistent with these sample types. Additionally, the changes observed in chemical
466 composition, emerging after 2 days of storage for a relatively small number of molecular
467 features, suggested these might be used as signature compounds for decomposition in meat
468 samples (Supplementary Figure 2).

Many known chemicals in tomatoes were detected, including chlorogenic acid derivatives and flavonoids (**Figure 5a**), both compound groups are found commonly in tomato cultivars (van der Hooft et al., 2012b; Floros et al., 2017). A molecular family of tomatidine-related molecules was observed in all tomato samples. Tomatidine, a tomato-specific alkaloid, as the name suggests, and structural component of related glycoalkaloids, is abundant in tomato plant leaves and stems but is less concentrated in the fruits. Similarly, phenylethyl pyranosides were observed in all tomatoes. Only in sundried tomatoes did we observe a spectral match with glucose, perhaps added as a sweetener. In both sundried and fresh tomatoes, we detected azoxystrobin, a fungicide used in agriculture. Many molecules, including added oils, sugars, and preservatives, might explain the differences observed between processed and raw tomatoes in the PCoA (Figure S1g, Figure 5a). 5'-methylthioadenosine, one source of ethylene, a ripening hormone in plants, was detected in all tomatoes, except sundried tomatoes (North et al., 2017). The relative concentrations of 5'-methylthioadenosine were observed to decrease over time/ripening (**Figure S2**).

483

484 *3.4 Molecular transformations*

Heatmaps as well as molecular networks, while very different but complementary visualization techniques, confirmed and complemented one another and provide additional perspectives to augment current food analysis. For example, theaflavin increased significantly in relative abundance over time, which was visualized in the heatmap (**Figure 4a,b**) as well as the molecular network displaying brewing time (**Figure S13**). In **Figure 6c**, theaflavin is associated with two unannotated compounds, which allowed the presence of two analogues with mass shifts of 16 and 30 Da to be confirmed and are consistent with a hydroxylated as

well as a double de-hydroxylated analogues, and other further reduced analogues. These kinds of relationships facilitate interpretation and understanding of chemical processes without requiring the identity of molecules detected to be known. The molecular composition of tea samples changed over time, with changes observed in the abundance consistent with continued extraction of molecules as opposed to chemical modifications. While a range of compounds increased in many of the varieties, there were molecular features specific to tea type, such as increased relative abundance of coniferyl aldehyde in only oolong tea (**Figure S6a** panel 2 and **Figure 6c** cluster 8). The molecular composition and extraction kinetics of oolong tea might differ from other varieties as a result of extensive drying, physical changes in the leaves (*e.g.* twisting/curling), and oxidation during production.

The changes observed in tea samples were in contrast to the yogurt samples, where chemical alterations over time varied significantly, likely due to microbial metabolism. We detected significant changes in PCoA, molecular networks, and heatmaps. In the PCoA, the home ferment inoculated with Kroger yogurt resembled the original starting culture, at a molecular level, and differed from other home ferments, possibly because it contained different yogurt cultures. Interestingly, when we focused our analysis on annotated compounds only, significant changes over time were not observed in the heatmap (**Figure 4** and **Figure S4**), indicating that many of the molecular transformations during fermentation have not been characterized yet or the reference spectra are not available in MS library databases. Consistent with the lack of reference spectra in public databases, the yogurt and milk samples also had the lowest annotation rate at 3.5%. Among the annotated features, we found a broad range of compounds (**Figure S8**), including food additives and sugars, which were also detected in other milk types within publicly available datasets on GNPS, such as

515 breast milk. The unexpected occurrence of bile acids in the milk and yogurt samples might
516 originate from secretion from the cows' mammary glands into the milk, as bile acids have
517 been detected previously in human breast milk (Forsyth et al., 1983).

518 **4. Conclusion**

519 Our study presents the first large-scale food composition analysis using mass spectral
520 molecular networking. The untargeted MS approach coupled with molecular networking
521 allowed us to assess large-scale differences between sample types, find molecule-molecule
522 links within and between sample types, and identify different compound classes found within
523 a sample type - all useful in biochemical interpretations and understanding. We determined
524 that foods undergo molecular changes caused by a variety of biological and chemical
525 processes over different time periods, as exemplified by meat, tea and yogurt. Brewing time
526 for tea altered its composition, increasing the diversity of molecules, whereas fermentation of
527 yogurt from milk, spoilage of meat, and ripening of tomatoes were all dominated by biological
528 transformations, altering the molecular composition over a longer period. Mass spectral
529 molecular networking and spectral library search successfully identified key molecular
530 features, which differed based on processing type, such as fermentation time in the yogurt
531 samples and brewing time for tea. Our study provides a reference dataset freely accessible
532 for feature mining in future food-related or other studies. One advantage of the GNPS
533 molecular networking workflow is the search parameter 'Find Related Datasets'. As shown in
534 this study, even the most traditional food types contain large numbers of unannotated
535 molecules and, therefore, we expect that increasing depositions of MS datasets in the public
536 domain would allow comparisons with other complex mixtures and narrow down the origins of

537 molecular features. This is the first large-scale food chemistry study, free and publicly
538 accessible through the KnowledgeBase GNPS (Wang et al., 2016). Anyone who wishes to
539 continue exploring these data can subscribe to the project, as it will be subject to living data
540 analysis. Living data is a strategy introduced to metabolomics in Wang et al. (2016), where
541 data are continuously re-analyzed, and updates are provided automatically to all subscribers.
542 This allows future studies to exploit the mass spectral molecular networking data with the
543 annotated food molecules, with the ability to propagate annotations across a new network to
544 better understand the chemical space that foods occupy and how food handling and
545 processing affect it. Given that 88-97% of all the MS/MS spectra are currently unannotated,
546 as a community, we will need to increase our knowledge about the molecular compositions
547 and molecular changes in our food. We have shown that, with our contribution to the food
548 chemistry field, GNPS molecular networking promises to become a key repository and
549 knowledgebase for untargeted MS-based food composition studies, and demonstrated the
550 utility of combining molecular networking approaches with statistical measures to discern
551 meaningful chemical transformations.

552

553 **Acknowledgments**

554 The result of this work was a part of a hands-on mass spectrometry course at UCSD called
555 “System Wide Mass Spectrometry”. The authors were all participants or mentors of this
556 course. We further acknowledge NIH number P41 GM103484, and NIH Grant
557 GMS10RR029121 and Bruker for the shared instrumentation infrastructure that enabled this
558 work and the UCSD Center for Microbiome Innovation. AMCR and PCD were supported by
559 NSF grant IOS-1656481. FV and PCD were supported by the Office of Naval Research

560 Multidisciplinary University Research Initiative (MURI) Award, Award number N000014-15-1-
561 2809.

562

563 **Appendix**

564 ***Supplementary data***

565 Supplementary data associated with this article can be found with the online version.

566 ***Data and code availability***

567 Data can be accessed via <http://gnps.ucsd.edu> via accession numbers for Milk/yogurt:

568 MSV000082387; Tea: MSV000082388; Coffee: MSV000082386; Meat: MSV000082423;

569 Tomato: MSV000082391. Metadata are uploaded with each dataset. All jupyter notebooks

570 and scripts used for data pre-processing and analysis are publically available at:

571 <https://github.com/DorresteinLaboratory/supplementary-MolecularChangesInFood>

572

573 Links to networking jobs for GNPS networking jobs: Parameters are precursor and fragment

574 ion tolerance set to 0.1 Da, min matched fragment ions: 4, cosine 0.7; library search min

575 match peaks: 4; run with metadata, attributes assigned; NIST17 included.

576 milk/yogurt samples only

577 <https://gnps.ucsd.edu/ProteoSAFe/status.jsp?task=1f11fb76e15240a893e46e02d9c58cd2>

578 tea samples only

579 <https://gnps.ucsd.edu/ProteoSAFe/status.jsp?task=f7569832b0d241f79812446d81cd5ca5>

580 coffee samples only

581 <https://gnps.ucsd.edu/ProteoSAFe/status.jsp?task=2c83502fefc0469ba79ba70a9461b9b5>

582 meat samples only

583 <https://gnps.ucsd.edu/ProteoSAFe/status.jsp?task=1520f7112d9f445384eb743ac4358c21>

584 tomato samples only

585 <https://gnps.ucsd.edu/ProteoSAFe/status.jsp?task=cf6e0347de8b48aeb8c700e45b4d3159>

586 All sample types:

587 <https://gnps.ucsd.edu/ProteoSAFe/status.jsp?task=b881151839574f639ceaf06f9b11e464>

588

589 Links for jobs performed to obtain the feature MS1 and MS/MS linked table for PCoA and

590 heatmaps and statistical analysis: Parameters are precursor and fragment ion tolerance set to

591 0.1 Da, 4 min match peaks, cosine 0.7; inputs are the .mgf; .csv from mzMINE and the

592 metadata file.

593 Global:

594 <https://gnps.ucsd.edu/ProteoSAFe/status.jsp?task=25577f11a35c48cdb30dfc005cbd6638>

595 milk/yogurt:

596 <http://gnps.ucsd.edu/ProteoSAFe/status.jsp?task=f9ede96d9e694f9e8b6186991e289c17>

597 tea:

598 <https://gnps.ucsd.edu/ProteoSAFe/status.jsp?task=80fc6384e52b4fe18e13ebbb3a86b4d8>

599 coffee:

600 <https://gnps.ucsd.edu/ProteoSAFe/status.jsp?task=750cc6fe82dc4732b84b355904cf91d3>

601 meat:

602 <https://gnps.ucsd.edu/ProteoSAFe/status.jsp?task=85c7380ca7ee44b3a3ed448c9b4d09fa>

603 tomato:

604 <http://gnps.ucsd.edu/ProteoSAFe/status.jsp?task=7a4031dd3ee146699ceecef919d7f668>

605 *Link to Clusterapp:*

606 <http://dorresteinappshub.ucsd.edu:3838/clusterMetaboApp0.9.1/>

607

608 **Conflict of interest statement**

609 Dorrestein is on the advisory board of Sirenas. NB was a co-founder, had an equity interest
610 and received income from Digital Proteomics, LLC through 2017. The terms of this
611 arrangement have been reviewed and approved by the University of California, San Diego in
612 accordance with its conflict of interest policies. Digital Proteomics was not involved in the
613 research presented here.

614

615 **References**

- 616 Aksenov, A. A., da Silva, R., Knight, R., Lopes, N. P., & Dorrestein, P. C. (2017). Global
617 chemical analysis of biology by mass spectrometry. *Nature Reviews Chemistry*, 1, 0054.
- 618 Berger, J., Roos, N., Greffeuille, V., Dijkhuizen, M., & Wieringa, F. (2019). Driving Policy
619 Change to Improve Micronutrient Status in Women of Reproductive Age and Children in
620 Southeast Asia: The SMILING Project. *Maternal and Child Health Journal*, 23(1), 79–85.
- 621 Blaženović, I., Kind, T., Ji, J., & Fiehn, O. (2018). Software tools and approaches for
622 compound identification of LC-MS/MS data in metabolomics. *Metabolites*, 8(2), 31.
- 623 Borges, R. M., Taujale, R., de Souza, J. S., de Andrade Bezerra, T., Silva, E. L. E., Herzog,
624 R., Ponce, F. V., Wolfender, J. L., & Edison, A. S. (2018). Dereplication of plant phenolics
625 using a mass-spectrometry database independent method. *Phytochemical Analysis*, (in
626 press) doi:10.1002/pca.2773.
- 627 Branen, A. L., Davidson, P. M., Salminen, S., & Thorngate, J. (2001). Food Additives. New
628 York: CRC Press. pp. 599–600. ISBN 9780824741709.
- 629 Brink, N. G., & Folkers, K. (1951). Isolation of Tomatidine from the Roots of the Rutgers
630 Tomato Plant. *Journal of the American Chemical Society*, 73(8), 4018.
- 631 Caporaso, J. G., Kuczynski, J., Stombaugh, J., Bittinger, K., Bushman, F. D., Costello, E. K.,
632 Fierer, N., Peña, A. G., Goodrich, J. K., Gordon, J. I., Huttley, G. A., Kelley, S. T., Knights,
633 D., Koenig, J. E., Ley, R. E., Lozupone, C. A., McDonald, D., Muegge, B. D., Pirrung, M.,
634 Reeder, J., Sevinsky, J. R., Turnbaugh, P. J., Walters, W. A., Widmann, J., Yatsunenko,
635 T., Zaneveld, J., & Knight, R. (2010). QIIME allows analysis of high-throughput community
636 sequencing data. *Nature Methods*, 7(5), 335–336.
- 637 Choi, J. H., Maeda, K., Nagai, K., Harada, E., Kawade, M., Hirai, H., & Kawagishi, H. (2010).
638 Termitomycamides A to E, fatty acid amides isolated from the mushroom *Termitomyces*
639 *titanicus*, suppress endoplasmic reticulum stress. *Organic Letters*, 12(21), 5012–5015.

- Clifford, M. N., Jaganath, I. B., Ludwig, I. A., & Crozier, A. (2017). Chlorogenic acids and the acyl-quinic acids: discovery, biosynthesis, bioavailability and bioactivity. *Natural Product Reports*, 34(12), 1391–1421.
- Cuyckens, F. & Claeys, M. (2004). Mass spectrometry in the structural analysis of flavonoids. *Journal of Mass Spectrometry*, 39(1), 1–15.
- Floros, D. J., Petras, D., Kaponov, C. A., Melnik, A. V., Ling, T.-J., Knight, R., & Dorrestein, P. C. (2017). Mass spectrometry based molecular 3D-cartography of plant metabolites. *Frontiers in Plant Science*, 8, 429.
- Forsyth, J. S., Ross, P. E. & Bouchier, I. A. D. (1983). Bile salts in breast milk. *Eur J Pediatr*, 140: 126-127.
- Friedman, M. (2013). Anticarcinogenic, Cardioprotective, and Other Health Benefits of Tomato Compounds Lycopene, α -Tomatine, and Tomatidine in Pure Form and in Fresh and Processed Tomatoes. *Journal of Agricultural and Food Chemistry*, 61(40), 9534–9550.
- Ge, Y. W., Zhu, S., Yoshimatsu, K., & Komatsu, K. (2017). MS/MS similarity networking accelerated target profiling of triterpene saponins in *Eleutherococcus senticosus* leaves. *Food Chemistry*, 227, 444–452.
- Giorio, C., Safer, A., Sánchez-Bayo, F., Tapparo, A., Lentola, A., Girolami, V., van Lexmond, M. B., & Bonmatin, J.M. (2017). An update of the Worldwide Integrated Assessment (WIA) on systemic insecticides. Part 1: new molecules, metabolism, fate, and transport. *Environmental Science and Pollution Research*. (in press) doi: 10.1007/s11356-017-0394-3.
- Granados-Chinchilla, F. & Rodríguez, C. (2017). Tetracyclines in food and feeding stuffs: From regulation to analytical methods, bacterial resistance, and environmental and health implications. *Journal of Analytical Methods in Chemistry*, 2017, 1315497.
- Islam, M. T., Tabrez, S., Jabir, N. R., Ali, M., Kamal, M. A., da Silva Araujo, L., De Oliveira Santos, J. V., Da Mata, A. M. O. F., De Aguiar, R. P. S., & de Carvalho Melo Cavalcante, A. A. (2018). An insight on the therapeutic potential of major coffee components. *Current Drug Metabolism*, (in press) doi: 10.2174/1389200219666180302154551.
- Luo, Z. M., Du, H. X., Li, L. X., An, M. Q., Zhang, Z. Z., Wan, X. C., Bao, G. H., Zhang, L., & Ling, T. J. (2013). Fuzhuanins A and B: the B-ring fission lactones of flavan-3-ols from Fuzhuan brick-tea. *Journal of Agricultural and Food Chemistry*, 61(28), 6982–6990.
- Lewis, J. E., Arheart, K. L., LeBlanc, W. G., Fleming, L. E., Lee, D. J., Davila, E. P., ... Clark, J. D. (2009). Food label use and awareness of nutritional information and recommendations among persons with chronic disease. *The American journal of clinical nutrition*, 90(5), 1351–1357.
- Marshall, J. W., Schmitt-Kopplin, P., Schuetz, N., Moritz, F., Roullier-Gall, C., Uhl, J., Colyer, A., Jones, L. L., Rychlik, M., & Taylor, A. J. (2018). Monitoring chemical changes during food sterilisation using ultrahigh resolution mass spectrometry. *Food Chemistry*, 242, 316–322.

- Naveed, M., Hejazi, V., Abbas, M., Kamboh, A. A., Khan, G. J., Shumzaid, M., Ahmad, F., Babazadeh, D., FangFang, X., Modarresi-Ghazani, F., WenHua, L., & XiaoHui, Z. (2018). Chlorogenic acid (CGA): A pharmacological review and call for further research. *Biomedicine & Pharmacotherapy*, 97:67–74.
- Nguyen, D. D., Wu, C. H., Moree, W. J., Lamsa, A., Medema, M. H., Zhao, X., Gavilan, R. G., Aparicio, M., Atencio, L., Jackson, C., Ballesteros, J., Sanchez, J., Watrous, J. D., Phelan, V. V., van de Wiel, C., Kersten, R. D., Mehnaz, S., De Mot, R., Shank, E. A., Charusanti, P., Nagarajan, H., Duggan, B. M., Moore, B. S., Bandeira, N., Palsson, B. Ø., Pogliano, K., Gutiérrez, M., & Dorrestein, P. C. (2013). MS/MS networking guided analysis of molecule and gene cluster families. *Proceedings of the National Academy of Sciences of the United States of America*, 110(28), E2611–E2620.
- North, J. A., Miller, A. R., Wildenthal, J. A., Young, S. J., & Tabita, F. R. (2017). Microbial pathway for anaerobic 5'-methylthioadenosine metabolism coupled to ethylene formation. *Proceedings of the National Academy of Sciences of the United States of America*, 114(48), E10455–E10464.
- Pastoriza, S., Mesías, M., Cabrera, C., & Rufián-Henares, J. A. (2017). Healthy properties of green and white teas: an update. *Food & Functions*, 8(8), 2650–2662.
- Scalbert, A., Brennan, L., Manach, C., Andres-Lacueva, C., Dragsted, L. O., Draper, J., Rappaport, S. M., van der Hooff, J. J. J., & Wishart, D. S. (2014). The food metabolome: a window over dietary exposure. *American Journal of Clinical Nutrition*, 99(6), 1286–1308.
- Scheubert, K., Hufsky, F., Petras, D., Wang, M., Nothias, L. -F., Dührkop, K., Bandeira, N., Dorrestein, P. C., & Böcker, S. (2017). Significance estimation for large scale metabolomics annotations by spectral matching. *Nature Communication*, 8(1), 1494.
- Shu, Y., Liu, J. Q., Peng, X. R., Wan, L. S., Zhou, L., Zhang, T., & Qiu, M. H. (2014). Characterization of diterpenoid glucosides in roasted puer coffee beans. *Journal of Agricultural and Food Chemistry*, 62(12), 2631–2637.
- Schulze, M. B., Manson, J. E., Ludwig, D. S., Colditz, G. A., Stampfer, M. J., Willett, W. C., ... Gimble, J. M. (2016). 2015 – 2020 Dietary Guidelines for Americans. *Am J Clin Nutr*.
- Sumner, L. W., Amberg, A., Barrett, D., Beale, M. H., Beger, R., Daykin, C. A., Fan, T. W.-M., Fiehn, O., Goodacre, R., Griffin, J. L., Hankemeier, T., Hardy, N., Harnly, J., Higashi, R., Kopka, J., Lane, A. N., Lindon, J. C., Marriott, P., Nicholls, A. W., Reilly, M. D., Thaden, J. J., & Viant, M. R. (2007). Proposed minimum reporting standards for chemical analysis. Chemical Analysis Working Group (CAWG) Metabolomics Standards Initiative (MSI). *Metabolomics*, 3(3), 211–221.
- Tajik, N., Tajik, M., Mack, I., & Enck, P. (2017). The potential effects of chlorogenic acid, the main phenolic components in coffee, on health: a comprehensive review of the literature. *European Journal of Nutrition*, 56(7), 2215–2244.
- Thirumdas, R., Brnčić, M., Brnčić, S. R., Barba, F. J., Gálvez, F., Zamuz, S., ... Lorenzo, J. M. (2018). Evaluating the impact of vegetal and microalgae protein sources on proximate

- composition, amino acid profile, and physicochemical properties of fermented Spanish “chorizo” sausages. *Journal of Food Processing and Preservation*, 42 (11), e13817
- Turman, M. V., Kingsley, P. J., Rouzer, C. A., Cravatt, B. F., & Marnett, L. J. (2008). Oxidative metabolism of a fatty acid amide hydrolase-regulated lipid, arachidonoyltaurine. *Biochemistry*, 47(12), 3917–3925.
- van der Hooft, J. J. J., Akermi, M., Ünlü, F. Y., Mihaleva, V., Roldan, V. G., Bino, R. J., de Vos, R. C., & Vervoort, J. (2012a). Structural annotation and elucidation of conjugated phenolic compounds in black, green, and white tea extracts. *Journal of Agricultural and Food Chemistry*, 60(36), 8841–8850.
- van der Hooft, J. J. J., Vervoort, J., Bino, R. J., & de Vos, R. C. H. (2012b). Spectral trees as a robust annotation tool in LC–MS based metabolomics. *Metabolomics*, 8(4), 691–703.
- Vázquez-Baeza, Y., Pirrung, M., Gonzalez, A., & Knight, R. (2013). EMPeror: a tool for visualizing high-throughput microbial community data. *Gigascience*, 2(1), 16.
- Wang, M., Carver, J. J., Phelan, V. V., Sanchez, L. M., Garg, N., Peng, Y., Nguyen, D. D., Watrous, J., Kapon, C. A., Luzzatto-Knaan, T., Porto, C., Bouslimani, A., Melnik, A. V., Meehan, M. J., Liu, W. T., Crusemann, M., Boudreau, P. D., Esquenazi, E., Sandoval-Calderón, M., Kersten, R. D., Pace, L. A., Quinn, R. A., Duncan, K. R., Hsu, C. C., Floros, D. J., Gavilan, R. G., Kleigrewe, K., Northen, T., Dutton, R. J., Parrot, D., Carlson, E. E., Aigle, B., Michelsen, C. F., Jelsbak, L., Sohlenkamp, C., Pevzner, P., Edlund, A., McLean, J., Piel, J., Murphy, B. T., Gerwick, L., Liaw, C. C., Yang, Y. -L., Humpf, H. U., Maansson, M., Keyzers, R. A., Sims, A. C., Johnson, A. R., Sidebottom, A. M., Sedio, B. E., Klitgaard, A., Larson, C. B., Boya P, C. A., Torres-Mendoza, D., Gonzalez, D. J., Silva, D. B., Marques, L. M., Demarque, D. P., Pociute, E., O'Neill, E. C., Briand, E., Helfrich, E. J. N., Granatosky, E. A., Glukhov, E., Ryffel, F., Houson, H., Mohimani, H., Kharbush, J. J., Zeng, Y., Vorholt, J. A., Kurita, K. L., Charusanti, P., McPhail, K. L., Nielsen, K. F., Vuong, L., Elfeki, M., Traxler, M. F., Engene, N., Koyama, N., Vining, O. B., Baric, R., Silva, R. R., Mascuch, S. J., Tomasi, S., Jenkins, S., Macherla, V., Hoffman, T., Agarwal, V., Williams, P. G., Dai, J., Neupane, R., Gurr, J., Rodríguez, A. M. C., Lamsa, A., Zhang, C., Dorrestein, K., Duggan, B. M., Almaliti, J., Allard, P. M., Phapale, P., Nothias, L. -F., Alexandrov, T., Litaudon, M., Wolfender, J. L., Kyle, J. E., Metz, T. O., Peryea, T., Nguyen, D. T., VanLeer, D., Shinn, P., Jadhav, A., Müller, R., Waters, K. M., Shi, W., Liu, X., Zhang, L., Knight, R., Jensen, P. R., Palsson, B. O., Pogliano, K., Lington, R. G., Gutiérrez, M., Lopes, N. P., Gerwick, W. H., Moore, B. S., Dorrestein, P. C., & Bandeira, N. (2016). Sharing and community curation of mass spectrometry data with Global Natural Products Social Molecular Networking. *Nature Biotechnology*, 34(8), 828–837.
- Watrous, J., Roach, P., Alexandrov, T., Heath, B. S., Yang, J. Y., Kersten, R. D., van der Voort, M., Pogliano, K., Gross, H., Raaijmakers, J. M., Moore, B. S., Laskin, J., Bandeira, N., & Dorrestein, P. C. (2012). Mass spectral molecular networking of living microbial colonies. *Proceedings of the National Academy of Sciences of the United States of America*, 109(26), E1743–E1752.

Yang, J. -Y., Sanchez, L. M., Rath, C. M., Liu, X., Boudreau, P. D., Bruns, N., Glukhov, E., Wodtke, A., de Felicio, R., Fenner, A., Wong, W. R., Linington, R. G., Zhang, L., Debonisi, H. M., Gerwick, W. H., & Dorrestein, P. C. (2013). Molecular networking as a dereplication strategy. *Journal of Natural Products*, 76(9), 1686–1699.

Yoshimura, Y., Goto-Inoue, N., Moriyama, T., & Zaima, N. (2016). Significant advancement of mass spectrometry imaging for food chemistry. *Food Chemistry*, 210, 200–211.

Zhang, S., Yang, C., Idehen, E., Shi, L., Lv, L., & Sang, S. (2018). Novel theaflavin-type chlorogenic acid derivatives identified in black tea. *Journal of Agricultural and Food Chemistry*, 66(13), 3402–3407.

Figure captions

Figure 1. Representative images of foods sampled and timeline of sampling. From top to bottom: Yogurt preparation from milk, brewed and loose leaf tea, different coffees, representing diverse roasts, brands and origins as ground coffee and brewed, ground beef and ground turkey left out to spoil, image from 3 days of storage depicted on the far right, and tomato types and ripening timeline. RT denotes room temperature and // denotes a time break. [color reproduction]

Figure 2. Global PCoA analysis to understand the molecular relationships among all samples analyzed. PC1 (10.43%); PC2 (5.96%); PC3 (5.86%). As a 2D image, the PCoA plot does not reveal the relationships clearly, a movie rotating this image is provided as supporting information [uploaded on massive.ucsd.edu MSV000083014]. MS1 features are TIC normalized per sample and the PCoA analysis was performed using Qiime1 and the Canberra distance metric. [color reproduction]

786 **Figure 3.** PCoA plots for the individual food types, color coded by metadata categories to
787 visualize key drivers in molecular patterns. The three store bought yogurts containing live
788 active cultures, the milk and the home ferments using the different yogurts as starter culture
789 show distinct groupings. The spheres are colored based on milk and yogurt type (a) or
790 fermentation time from 0 to 58 hrs (b). Tea samples differentiated based on tea type and
791 brewed tea vs. tea leaves (c). The time course of tea extraction is displayed for American and
792 British teas: black, green, matcha green, and white teas (d). [color reproduction]

793

794 **Figure 4.** Metabolites changing over tea extraction time and during the fermentation process
795 from milk to yogurt. a) Heatmap showing tea metabolites changing over extraction time
796 across different tea types. b) Specific metabolites increase significantly in their relative
797 intensity during tea extraction time. c) Heatmap showing metabolites changing during the
798 fermentation process from milk to yogurt across different yogurt brands used as inocula, as
799 well as the milk as control. d) Metabolites increasing or decreasing significantly during the
800 fermentation process across different home ferments. Metabolite annotation was performed
801 through mass spectral molecular networking and spectral matching to reference spectra.
802 [color reproduction]

803

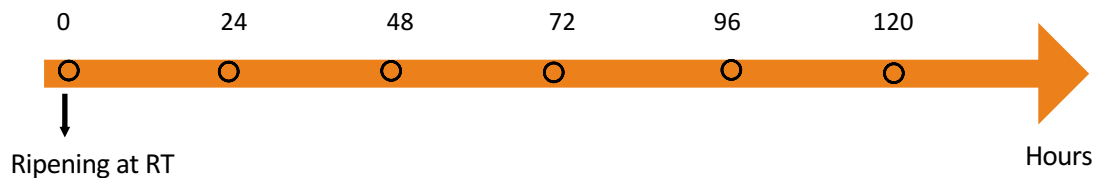
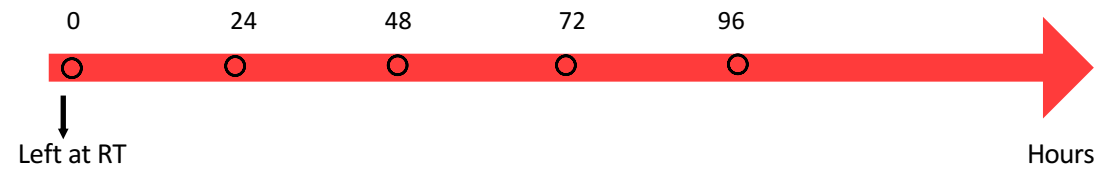
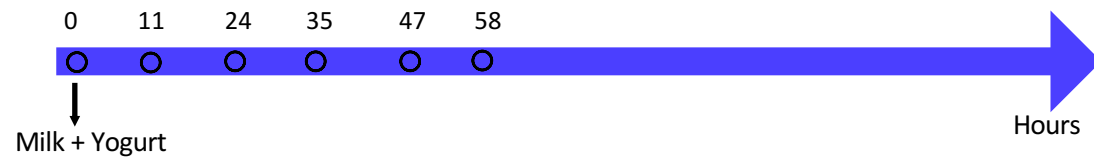
804 **Figure 5.** Molecular network clusters of the a) tomato color coded by processing method, b)
805 milk to yogurt, c) coffee data. The clusters are enlarged regions of specific molecular families
806 observed within the full molecular network. The color coding for different samples groups are
807 explained in the figure legend. Node sizes indicated relative precursor abundance and
808 selected library identifications are annotated in the figure and shown through squared node

809 shape. The full size images of the entire network where one can zoom in to the molecular
810 networks can be found as supporting information (**Figure S7-S9**) and the GNPS links to the
811 analysis jobs are provided in the data availability section. All annotations shown are level 2 or
812 3 according to the 2007 metabolomics standards guidelines (Sumner et al., 2007). [color
813 reproduction]

814

815 **Figure 6.** Molecular networks of the data. a) reflect the meat samples color coded by turkey
816 or beef. b) same network as a) but color coded by aging time. c) molecular networks color
817 coded by tea. The clusters are enlarged regions of specific molecular families observed within
818 the full molecular network. The full size images of the entire molecular networks where one
819 can zoom in molecular networks can be found as supporting information (**Figures S10-S12**)
820 and the GNPS links to the analysis jobs are provided in the data availability section. All
821 annotations shown are level 2 or 3 according to the 2007 metabolomics standards guidelines
822 (Sumner et al., 2007). [color reproduction]

823



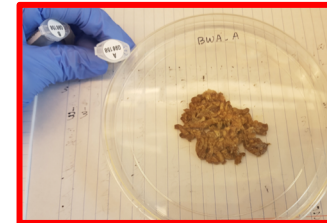
1 whole milk (Horizon Organic Vitamin D Milk)
3 brands of yogurt: Oikos plain Greek nonfat , Voskos plain Greek , Kroger plain nonfat Greek



6 tea types:
White, Green, Pu'er
Matcha Green ,
Oolong, Black



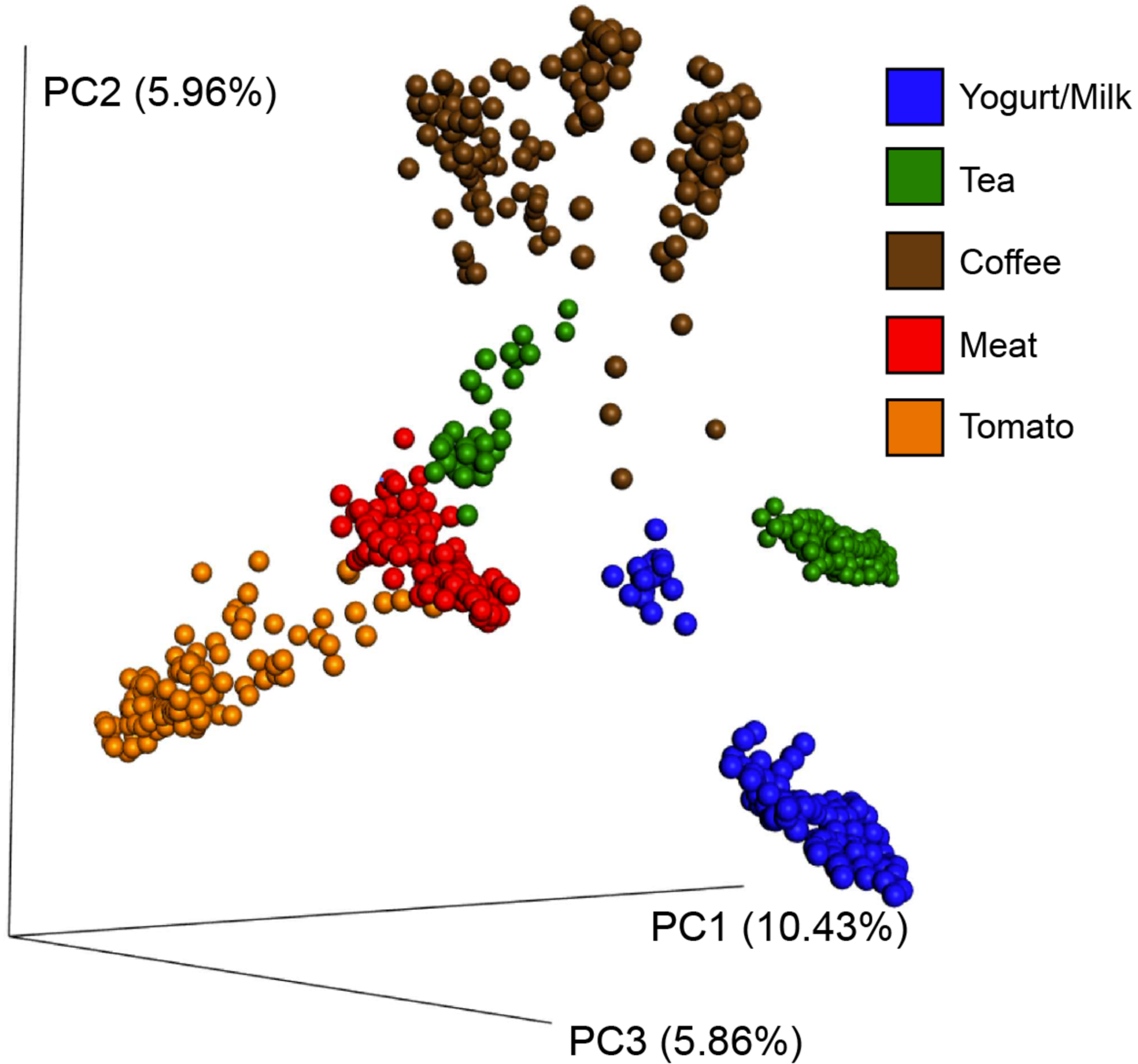
38 varieties of coffee
different roast, brand
and origin

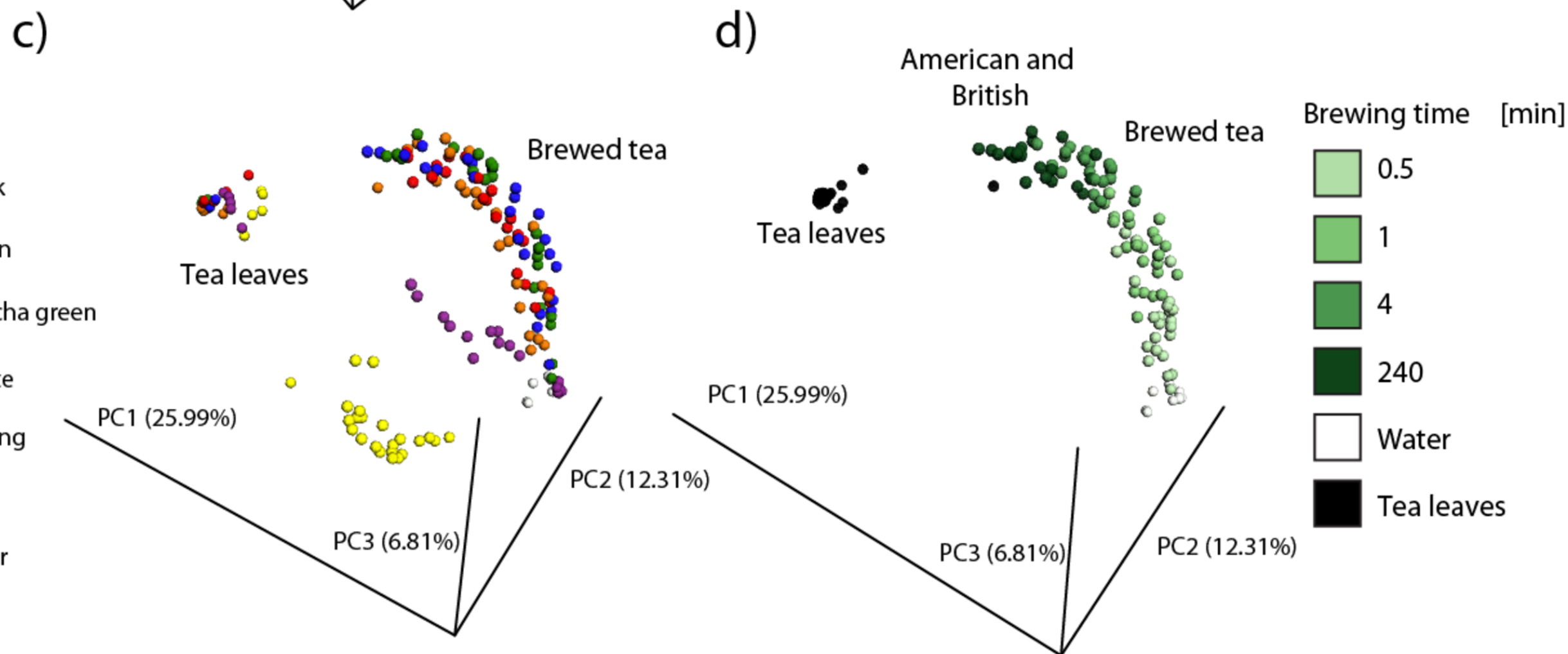
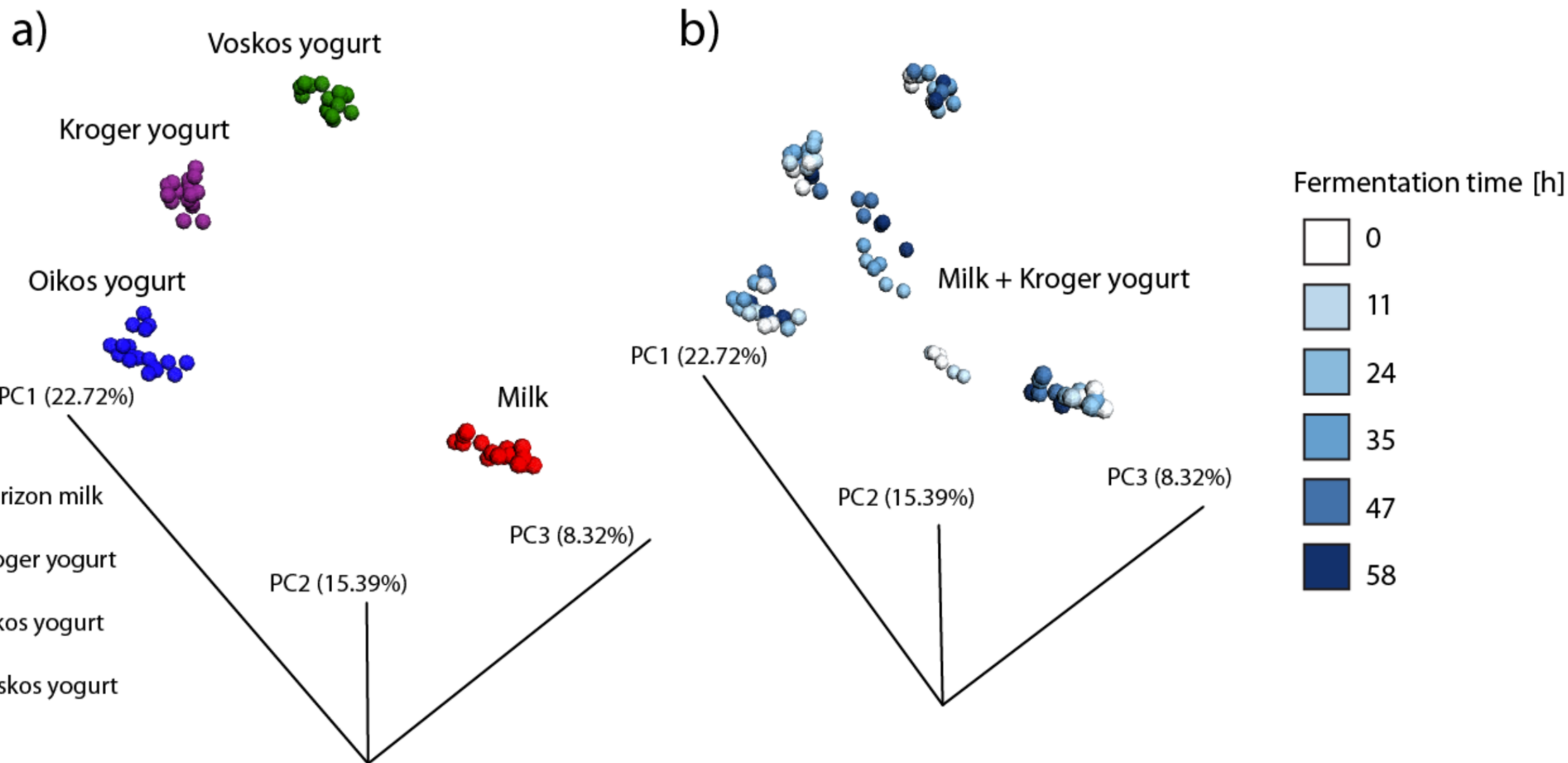


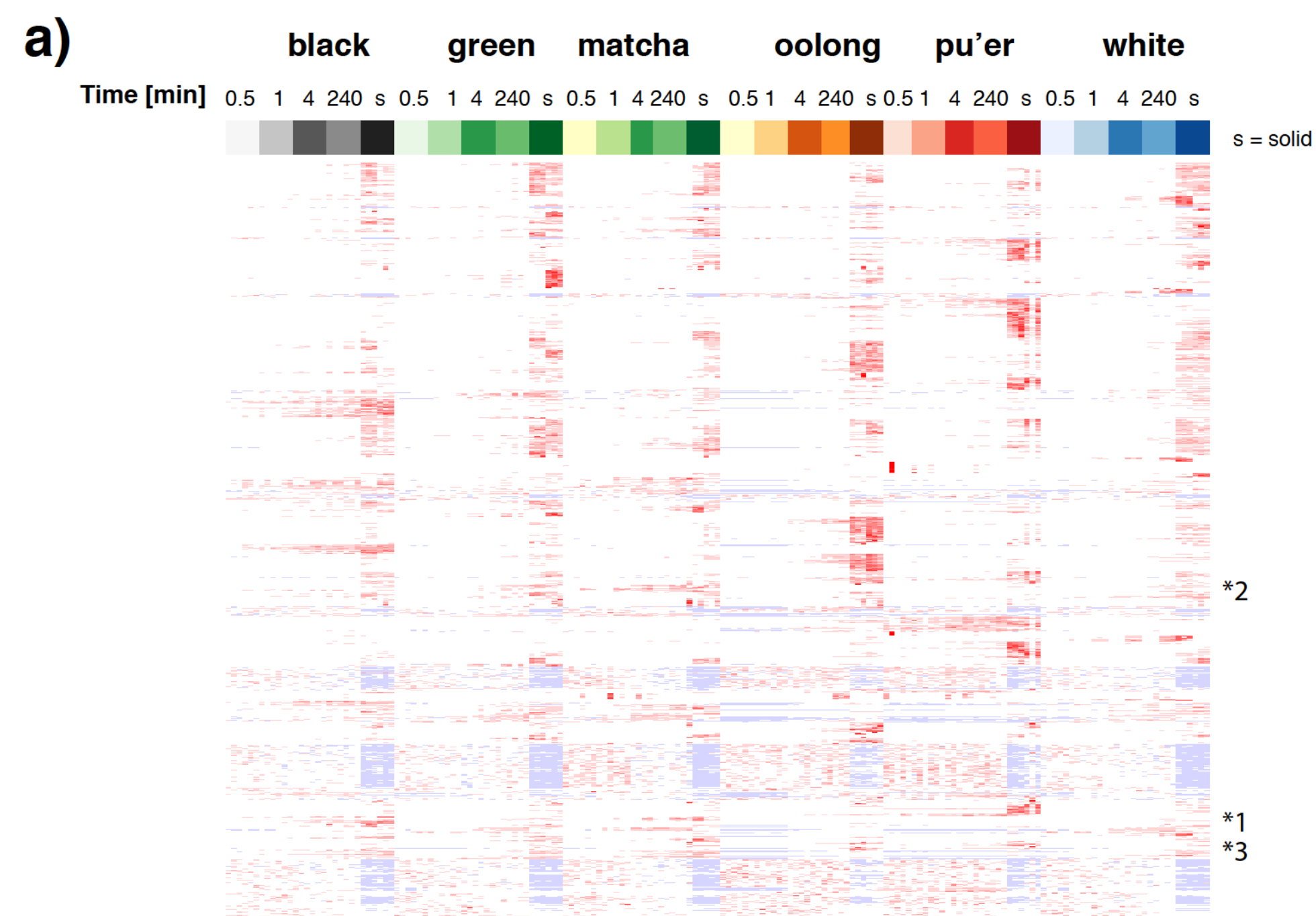
4 types of meat :
Ground Beef
Ground Beef (certified organic)
Ground Turkey
Ground Turkey (certified organic)



Organic cherry tomatoes
Non organic cherry tomatoes
Sun-dried tomatoes
Canned tomatoes

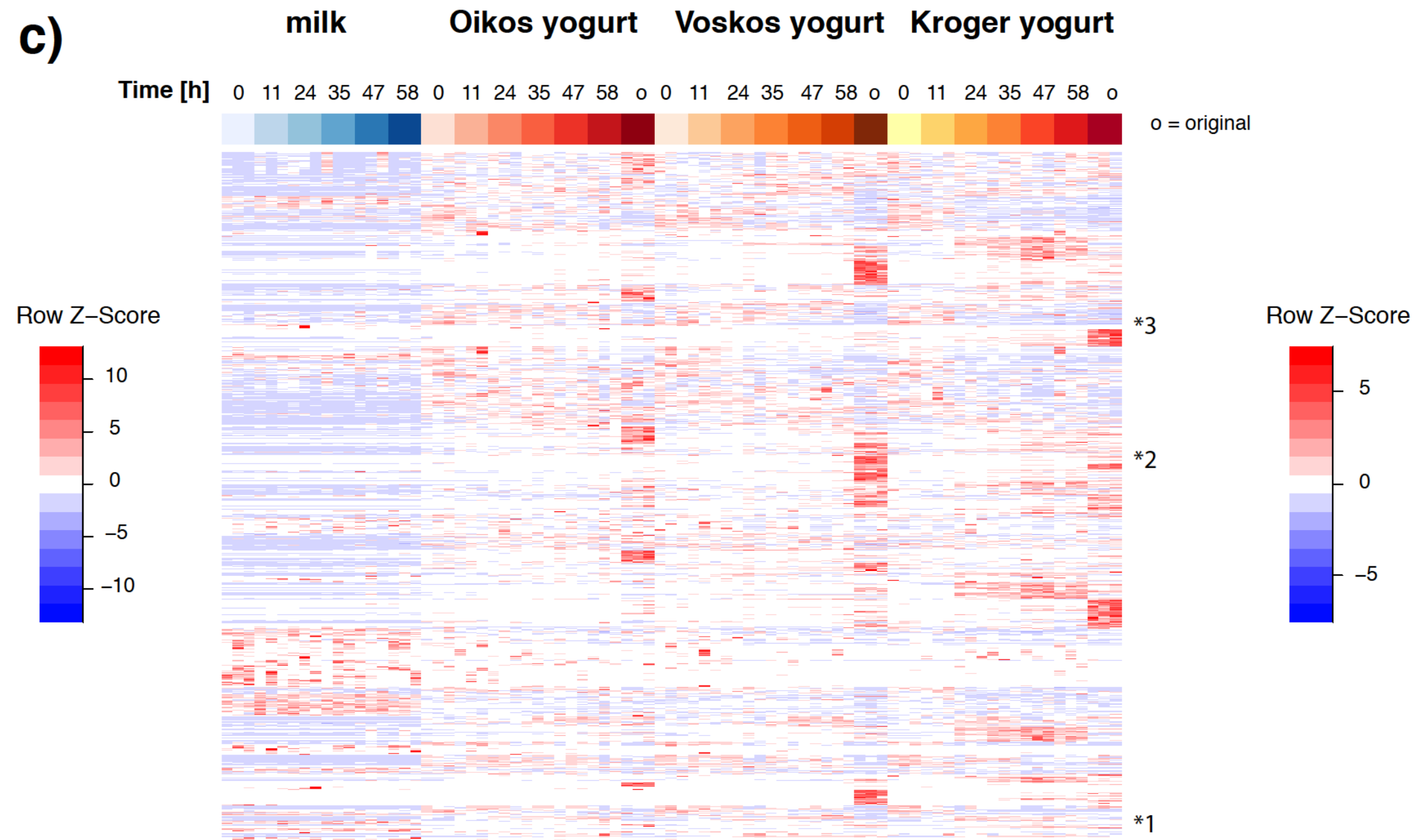
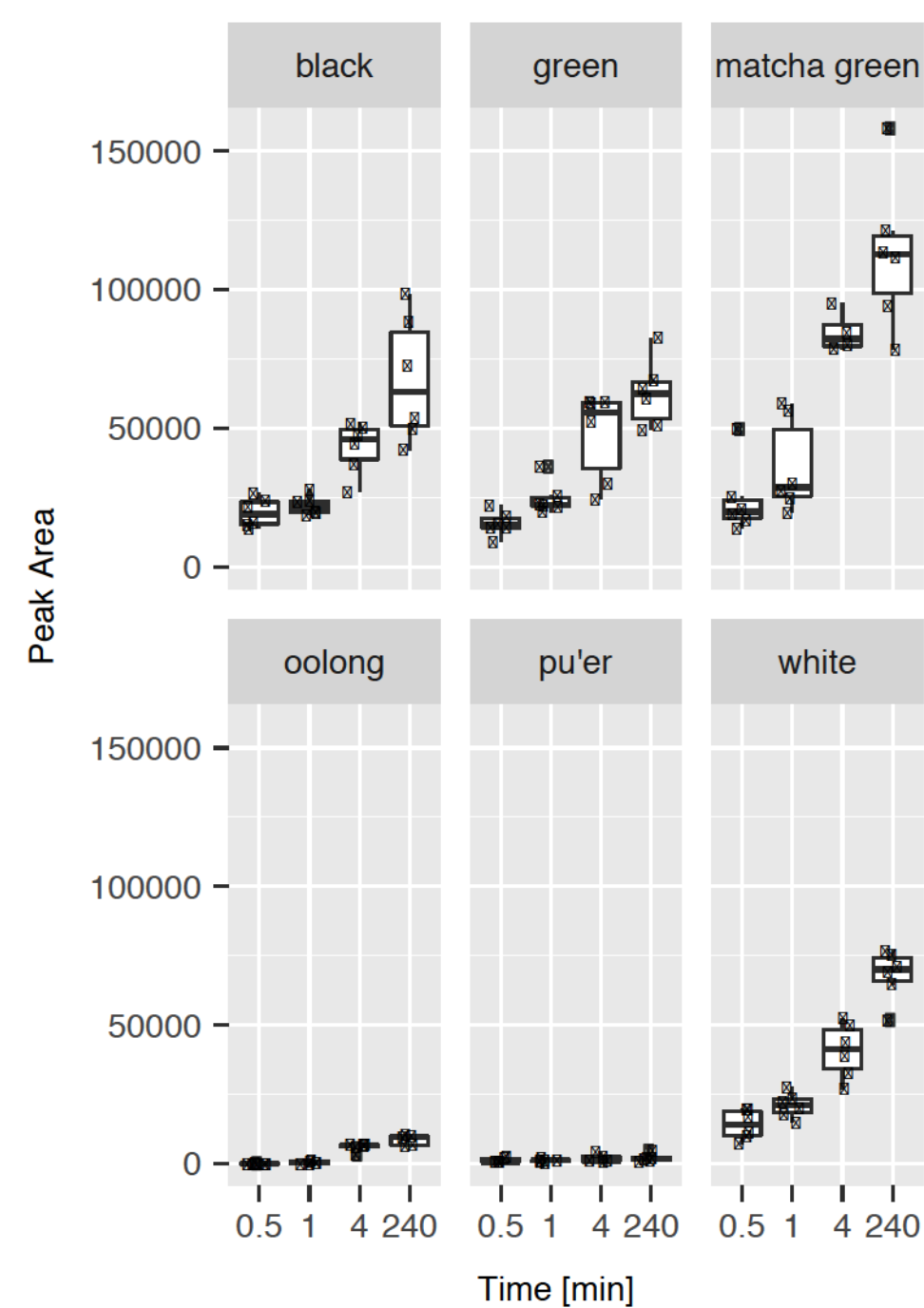






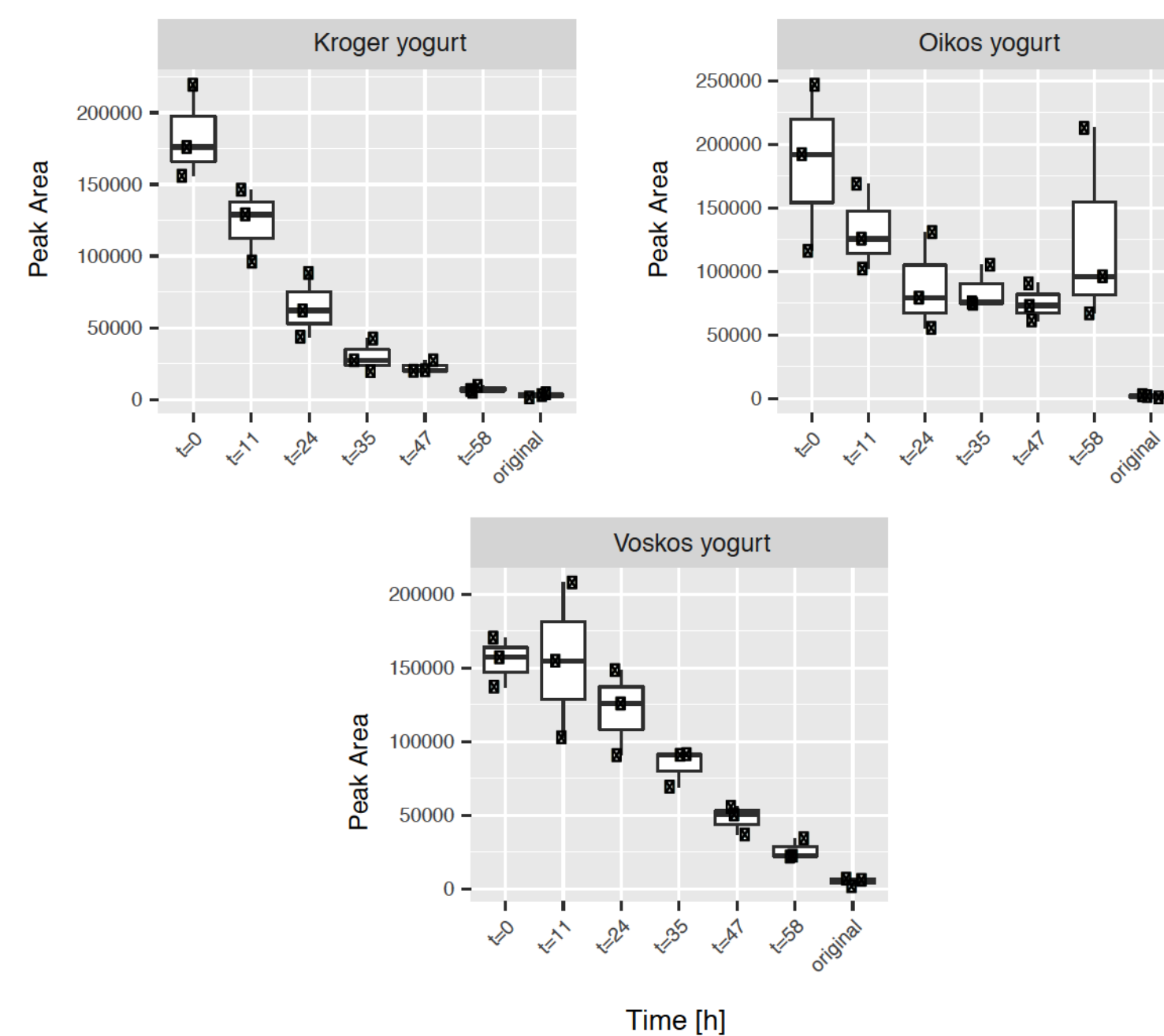
b)

1. Theaflavin

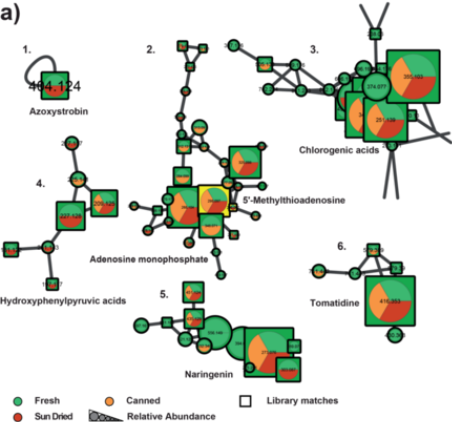


d)

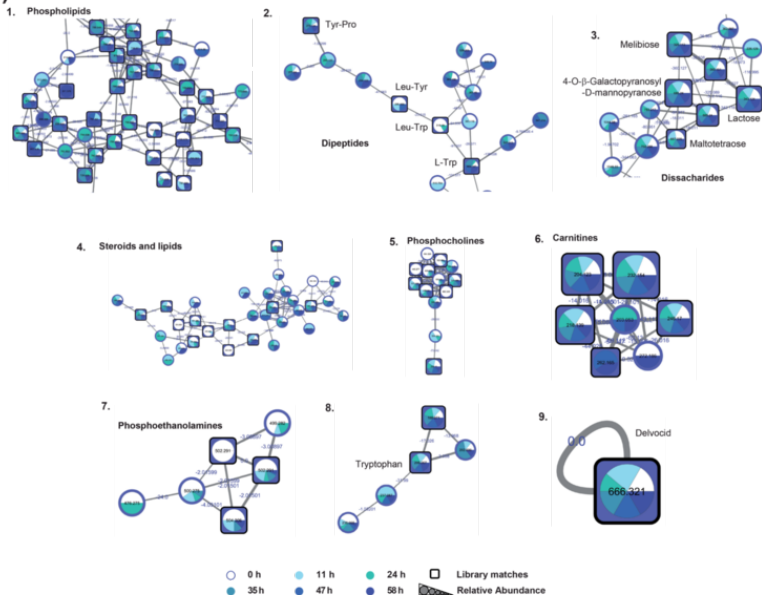
1. 4-*O*-beta-Galactopyranosyl-*D*-mannopyranose



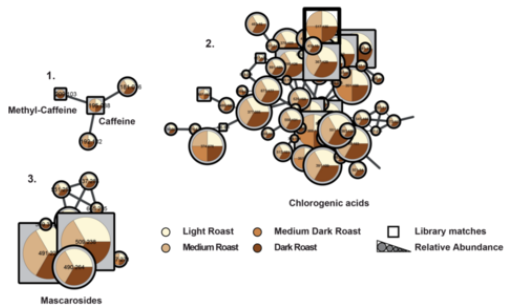
a)



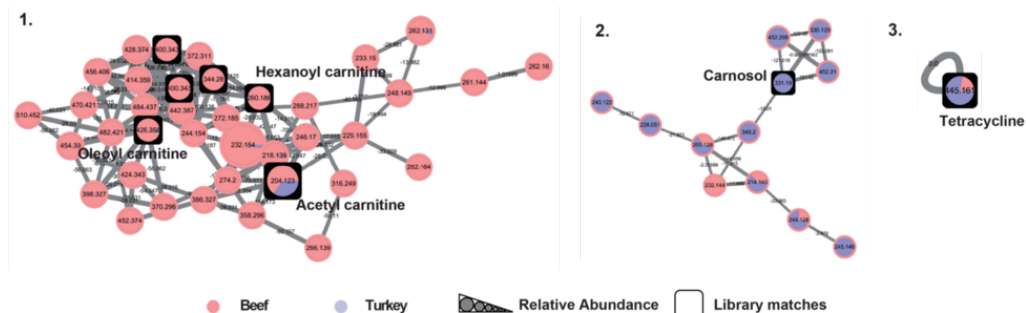
b)



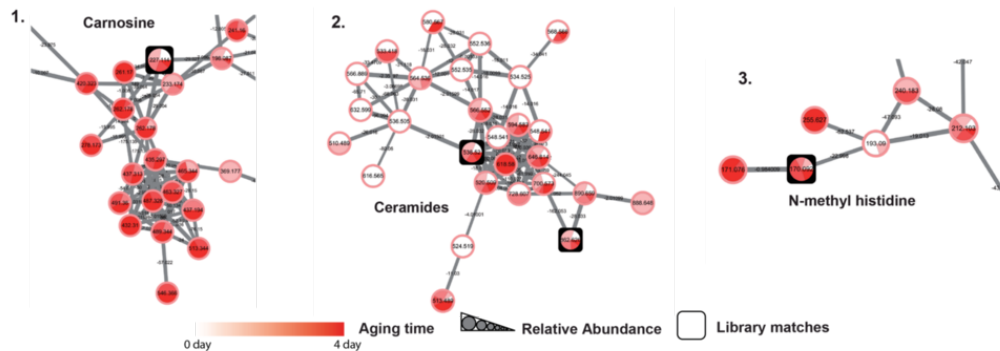
c)



a)



b)



c)

